

# Variable Structure Position Control of an Industrial Robotic Manipulator

**M. F. Mendes**

Universidade Estadual do Oeste do Paraná  
Centro de Engenharias e Ciências Exatas  
CECE UNIOESTE  
85857-970 Foz do Iguaçu, PR, Brazil  
mendes@ieee.org

**W. Kraus Jr.**

Universidade Federal de Santa Catarina  
Departamento de Automação e Sistemas  
DAS CTC UFSC  
88040-900 Florianópolis, SC, Brazil  
werner@das.ufsc.br

**E. R. de Pieri**

Universidade Federal de Santa Catarina  
Departamento de Automação e Sistemas  
DAS CTC UFSC  
88040-900 Florianópolis, SC, Brazil  
edson@das.ufsc.br

*The use of a robust position controller for a robotic manipulator moving in free space is presented. The aim is to implement in practice a controller that is robust to uncertainties in the model of the system, as well as being inexpensive from a computational point of view. Variable structure theory provides the technique for the design of such controller. The design steps are presented, first from a theoretical perspective and then applied to the control of a two degree-of-freedom manipulator. Simulation results that backed the implementation are presented, followed by the experiments conducted and the results that were obtained. The conclusion is that variable structure control is readily applicable to industrial robots for the robust control of positions.*

**Keywords:** Robotic manipulators, position control, variable structure control

## Introduction

Most industrial applications of robot manipulators use position control. Examples include spray painting, spot welding and pick-and-place operations. In such tasks, the aim is to have the manipulator following a path (position and orientation) in free space with timing restrictions. Such a timed path is called a *trajectory* of the *end effector* of the manipulator. By definition, trajectories in free space do not introduce contact forces between the manipulator and its environment.

The problem with present-day industrial position controllers is the performance deterioration when faster trajectories are demanded. To solve this problem, the paper describes the application of a variable structure (VS) controller to the control of a SCARA industrial manipulator. The contribution is in the demonstration of the viability of such control method in industrial robots and the confirmation of the capabilities of VS control promised by theoretical and experimental results.

The literature presents several approaches for the position control of manipulators. Among them, the most used controllers are computed-torque, proportional-plus-derivative (PD), PD plus integral action (PID) and PD with gravity compensation (Canudas, Siciliano and Bastin, 1996; Lewis, Abdallah and Dawson, 1993). These so-called "classical controllers" (PD and PID) do not present adequate performance when trajectories with severe timing restrictions (i.e., high velocities and accelerations) have to be performed.

Due to performance limitations of classical controllers, the computed torque strategy is usually desirable in advanced applications. It consists of the computation of torques that would cancel the natural dynamics of the mechanical linkage of the manipulator and, as such, requires a precise knowledge of the mathematical model of the manipulator. This model consists of differential equations that provide the relationship between the

torques applied at the joints and the resulting accelerations. To obtain the model, it is necessary the knowledge of the manipulator's masses, the geometry of the links and, eventually, the load being carried, which are not always available with the necessary accuracy. Besides, there are dynamic effects that are difficult to capture in the model, such as those introduced by friction and by the modes of vibration of the manipulator links and joints (which are not perfectly rigid). Such modeling difficulties cause the computed-torque strategy to present poor robustness to parametric uncertainties and unmodeled dynamics.

Modeling difficulties introduce the need for a robust controller with regard to the uncertainties in the model. There are many known methods for this purpose, as, for instance,  $H_2$  and  $H_\infty$  design (Doyle et al., 1989), and two-degree-of-freedom control (Wolovich, 1995). These methods have a common feature: the need for a linearized model and the high computational cost. This makes their use unfeasible for real-time control of a highly nonlinear mechanism as a robotic arm. To provide robustness to a manipulator's control system, the implementation of a controller using the VS control approach (Utkin, 1992) is proposed in this paper. VS control implements a nonlinear control law that accomplishes high-speed switchings on a surface specified in the state space containing the equilibrium point of the system. Experimental results show that VS control can be readily deployed in industrial robots.

The paper is structured as follows. Next section introduces the mathematical modeling of a robot manipulator. The third and fourth sections present the VS theory and a methodology for the design of a position controller applied to a robot manipulator in joint space using sliding modes. The fifth and sixth sections show simulation and experimental results from the use of VS control in a SCARA robot manipulator. The last section shows the concluding remarks and future directions.

## Dynamic Model of the Robotic Manipulator

The dynamic equation in the joint space for a robot manipulator with  $n$  degrees of freedom can be written as (Asada & Slotine, 1986):

$$H(q)\ddot{q} + C(q, \dot{q})\dot{q} + G(q) = u \quad (1)$$

where  $q$  is the vector ( $n \times 1$ ) of generalized coordinates (joint positions),  $H(q)$  is the ( $n \times n$ ) inertia matrix,  $C(q, \dot{q})$  is the ( $n \times n$ ) matrix of centripetal and coriolis forces,  $G(q)$  is the ( $n \times 1$ ) vector of gravitational forces and  $u$  is the ( $n \times 1$ ) vector of torques (the control inputs).

This model does not take into account actuators' dynamics (motors and gearboxes), as well as friction forces. Besides, the robot is considered rigid, i.e., without flexibility in the links and in the joints (Canudas, Siciliano and Bastin, 1996; Lewis, Abdallah and Dawson, 1993). With these assumptions, the obtained model is simpler and represents well the manipulator for the purpose of this paper, once the goal is the design of a controller that provides robustness to the system despite inaccuracies in the model.

## Variable Structure Control

Russian authors initially proposed the VS theory in the 60's using the mathematical work of Filippov (Filippov, 1964). Several authors have been studying it, both in *continuous time* (DeCarlo, Zak and Matthews, 1988, El-Khazali and DeCarlo, 1995, Fu and Liao, 1990, Utkin, 1992) and in *discrete time* (Gao, Wang and Homaifa, 1995). The aim of these works is the robust control of many kinds of nonlinear systems, among them the object of our study: robotic manipulators.

VS controllers provide an effective and robust way for controlling nonlinear plants and its roots are the *bang-bang* and *relay control theory* (DeCarlo, Zak and Matthews, 1988). The term VS control arose because the controller's structure is intentionally changed according with some rule to obtain the desired plant behavior. Due to this structure change, the resulting control law is nonlinear.

The rule that governs the change of the controller structure is given by functions of the state variables chosen by the designer. When equated to zero, these functions define a surface in the state space called *sliding surface* (some authors call it *switching surface*) (DeCarlo, Zak and Matthews, 1988; Utkin, 1977; Utkin, 1983) that governs the switching of the controller.

The control law aims at keeping the *system state* moving on this surface until reaching the equilibrium point, even in the presence of parametric uncertainties and disturbances. The property of the system state remaining on "sliding" in this surface is called *sliding mode*.

This control strategy presents two great advantages for applications in robotic manipulators:

- the exact knowledge of the manipulator's model is not needed;
- under certain conditions, the system performance is insensitive to bounded external disturbances.

These properties are important because the calculation of the exact manipulator dynamics is difficult, as discussed before. Besides, the effect of attaching loads to the manipulator's end effector can be considered as external disturbances in the design of the controller.

The first step in designing a VS controller is the choice of a set of  $m$  system state vector functions:

$$s_i(x, t) \quad ; \quad i = 1, \dots, m. \quad (2)$$

Equating this set of functions to zero:

$$s(x, t) = \begin{bmatrix} s_1(x, t) \\ s_2(x, t) \\ \vdots \\ s_m(x, t) \end{bmatrix} = 0, \quad (3)$$

the sliding surface is obtained. The functions (2) are designed so that the original system, restricted to the intersection of these surfaces, presents the desired dynamic behavior. Figure 1 shows an example of a sliding surface for two state vector functions. The "surface" in the figure is actually a line, representing the intersection of the planes defined by the switching functions.

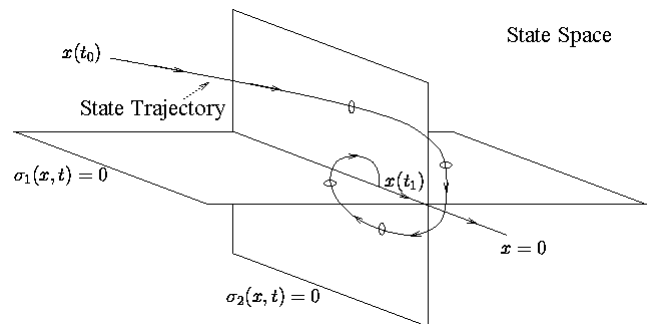


Figure 1. Sliding Surface.

A more convenient form for the design of a sliding surface is to suppose that the system is in the *regular form* (DeCarlo, Zak and Matthews, 1988, Utkin, 1977, Utkin, 1983). If this is not the case, then a nonlinear transformation needs to be applied on the original system. In both cases, the nonlinear system in regular form is given by:

$$\begin{aligned} \dot{x}_1 &= f_1(x, t) \\ \dot{x}_2 &= f_2(x, t) + B_2(x, t)u(x, t) \end{aligned} \quad (4)$$

where  $x_1$  and  $x_2$  are of dimensions  $((n - m) \times 1)$  and  $(m \times 1)$ , respectively. In this form, it is seen that the control  $u(x, t)$  enters in the partition  $x_2$  of the state.

The regular form can be obtained through linear transformations or, in some cases, through a nonlinear transformation. In the case of linear systems, a transformation that takes the system to the regular form always exists. For nonlinear systems, the existence of this transformation is not guaranteed (DeCarlo, Zak and Matthews, 1988). Fortunately, the nonlinear dynamic equation (1) that describes the behavior of a robotic manipulator can always be transformed to the regular form.

Given a system in regular form (4), the sliding surface (3) can be written as:

$$s(x, t) = Kx + r(t) = \begin{bmatrix} K_1 & K_2 \end{bmatrix} \cdot \begin{bmatrix} x_1 \\ x_2 \end{bmatrix} + r(t) = 0 \quad (5)$$

where  $K$  is a gain matrix chosen so that  $K_2$  is not singular, and  $r(t)$  is a reference signal to be tracked.

The effect of the VS control can be seen by making  $r(t) = 0$ . In this case, the behavior of the system during the sliding phase is given by:

$$s(x, t) = Kx = \begin{bmatrix} K_1 & K_2 \end{bmatrix} \cdot \begin{bmatrix} x_1 \\ x_2 \end{bmatrix} = 0 \quad (6)$$

so that

$$x_2 = -K_2^{-1}K_1x_1 \quad (7)$$

and the dynamics of the system is given by a reduced order model with dimension  $m$ . Also, when  $x_1$  goes to zero,  $x_2$  vanishes.

The dynamics of this nonlinear system can be changed such that the desired behavior during the sliding phase is obtained, through a convenient selection of the gain matrix  $K$ .

The second phase of the controller design consists of the determination of the switched control law that causes the system state to be attracted to the sliding surface. Upon reaching this surface, the state is kept there by the VS control until the system equilibrium is reached. For this end, the controller signal must be designed so that the vectors tangent to the state trajectory point towards the surface (DeCarlo, Zak and Matthews, 1988, Utkin, 1977, Utkin, 1983).

A control law that complies with the above requisite is the switched law:

$$u_i = -u_{0i} \operatorname{sgn}(s_i(x, t)) = \begin{cases} -u_{0i} & , \text{if } s_i(x, t) > 0 \\ 0 & , \text{if } s_i(x, t) = 0 \\ +u_{0i} & , \text{if } s_i(x, t) < 0 \end{cases} \quad (8)$$

where  $u_{0i}$  is the absolute value of the maximum signal control for the input  $i$ . Notice that regardless of the values of the state variables and gain  $K$  in Eq. (6), the control action  $u_i(x, t)$  is limited to  $\pm u_{0i}$ .

In practice, the VS control introduces a problem. An *ideal sliding mode* (Utkin, 1977) will exist only when the state trajectory is confined to the sliding surface, i.e., when  $s(x, t)$  is identically zero for  $t \geq t_1$  for some  $t_1$ . However, due to physical limitations of the actuators such as, for example, *delay*, *dead zone* and *hysteresis*, it is impossible to achieve an extremely fast switching, so that an ideal sliding mode is not reached.

Due to this limitation, a high frequency noise arises in the control action when the system state is close to the sliding surface. This phenomenon is known as *chattering* (DeCarlo, Zak and Matthews, 1988, El-Khazali and DeCarlo, 1995, Utkin, 1977):

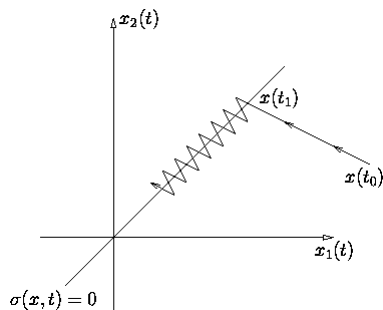


Figure 2. The Chattering phenomenon near a sliding surface.

Chattering makes the system state oscillate around the sliding surface, as showed in Fig. 2 and introduces two problems in control systems:

- the non-modeled high frequency dynamics can be excited, resulting in unforeseen unstable behavior;
- the actuators are placed under undue stress, so their breakages can take place or their lifetime are reduced.

To solve this problem, a continuous control law that approaches the discontinuous law operation close to the switching surface region can be used, obtaining thus a reference tracking with controlled accuracy. There is a tradeoff relationship between the level of chattering in the control signal and the accuracy in reference tracking: the more exact the tracking of references, the higher the level of chattering.

Using the *boundary layer* concept (DeCarlo, Zak and Matthews, 1988, Slotine and Li, 1991, Utkin, 1977), it can be shown that sliding occurs along a neighborhood of size equal to  $2\epsilon$  of the sliding surface defined as:

$$\{ x \mid |s(x, t)| \leq \epsilon \} \quad (9)$$

where  $\epsilon > 0$ .

Figure 3 shows the system state behavior when a boundary layer is used.

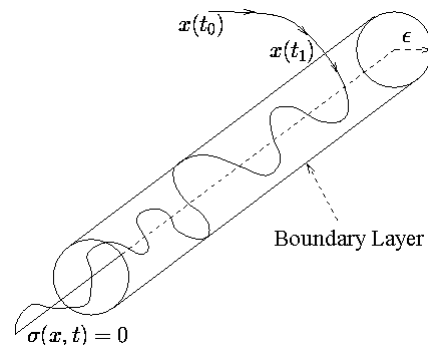


Figure 3. Boundary layer enclosing the sliding surface.

To implement the boundary layer, the function  $\operatorname{sgn}(\cdot)$  in Eq. (8) is changed to:

$$\operatorname{sat}(x / \epsilon) = \begin{cases} \operatorname{sgn}(x) & , \text{if } |x| \geq \epsilon \\ \frac{x}{\epsilon} & , \text{if } |x| < \epsilon \end{cases} \quad (10)$$

Thus, an infinitely fast commutation (8) is replaced by a softer commutation. With this modification in the control law, the system state trajectory confined to the boundary layer is only an approximation of the desired state trajectory along the sliding surface. Thus, asymptotic stability is not guaranteed, but only the stability in a region of radius  $\epsilon$  from the equilibrium point. Note that the smaller the values of  $\epsilon$ , the closer the system will be to the ideal sliding mode.

## Synthesis of the Controller

The objective here is the control of the position and velocity of the joints of a robotic manipulator. To this end, the design of the control law considers the manipulator's joints independently, that is, without coupling among them. Thus, each joint is controlled as a

system with one input and one output, and the coupling is treated as an external disturbance.

For the development of the controller, the following state variables are used:

$$\begin{bmatrix} \mathbf{q} \\ \mathbf{w} \end{bmatrix} = \begin{bmatrix} \mathbf{q} \\ \dot{\mathbf{q}} \end{bmatrix} \quad (11)$$

where  $\mathbf{q}$  and  $\mathbf{w}$  are the joints positions and velocities, respectively.

Considering that the gravitational forces term  $G(q)$  can be computed with great accuracy in real time, so that it can be eliminated of Eq. (1), the system model can be expressed with state equations in the regular form (4):

$$\begin{bmatrix} \dot{\mathbf{q}} \\ \dot{\mathbf{w}} \end{bmatrix} = \begin{bmatrix} 0 & I \\ 0 & -H^{-1}(q)C(q, \dot{q}) \end{bmatrix} \cdot \begin{bmatrix} \mathbf{q} \\ \mathbf{w} \end{bmatrix} + \begin{bmatrix} 0 \\ H^{-1}(q) \end{bmatrix} \cdot u, \quad (12)$$

or:

$$\begin{aligned} \dot{q}_1 &= f_1(q, \dot{q}, t) = \begin{bmatrix} 0 & I \end{bmatrix} \cdot \begin{bmatrix} q \\ \dot{q} \end{bmatrix} \\ \dot{q}_2 &= f_2(q, \dot{q}, t) + B_2(q, \dot{q}, t)u = \begin{bmatrix} 0 & H^{-1}(q)C(q, \dot{q}) \end{bmatrix} \cdot \begin{bmatrix} q \\ \dot{q} \end{bmatrix} + \begin{bmatrix} H^{-1}(q) \end{bmatrix} \cdot u \end{aligned} \quad (13)$$

The objective is to control the joints' positions and velocities; thus, a natural choice for the sliding surface is:

$$\mathbf{s}(\mathbf{q}, \mathbf{w}, t) = \begin{bmatrix} K_1 & K_2 \end{bmatrix} \cdot \begin{bmatrix} \mathbf{q} \\ \mathbf{w} \end{bmatrix} + r(t) \quad (14)$$

where  $K_1$  and  $K_2$  are strictly positive diagonal matrices and  $r(t)$  is a reference signal to be tracked or regulated. Each element of the vector  $\mathbf{s}(\mathbf{q}, \mathbf{w}, t)$  (14) can be expressed as:

$$\mathbf{s}_i(\mathbf{q}_i, \mathbf{w}_i, t) = k_{1i}\mathbf{q}_i + k_{2i}\mathbf{w}_i + r_i(t). \quad (15)$$

Considering that the desired position of the joint  $i$ ,  $\mathbf{q}_{di}$  (continually differentiable and limited) is a solution of this equation, the reference signal  $r_i(t)$  is given by:

$$r_i(t) = -k_{1i}\mathbf{q}_{di} - k_{2i}\mathbf{w}_{di} \quad (16)$$

where  $\mathbf{w}_{di}$  is the first temporal derivative of the desired position  $\mathbf{q}_{di}$ .

Replacing the reference  $r_i(t)$  (16) in Eq. (15) gives:

$$\mathbf{s}_i(\mathbf{q}_i, \mathbf{w}_i, t) = k_{1i}(\mathbf{q}_i - \mathbf{q}_{di}) + k_{2i}(\mathbf{w}_i - \mathbf{w}_{di}). \quad (17)$$

Defining the negative error vectors for the position and velocity of the joints as:

$$\tilde{\mathbf{q}} = \mathbf{q} - \mathbf{q}_d \quad (18)$$

and:

$$\tilde{\mathbf{w}} = \mathbf{w} - \mathbf{w}_d \quad (19)$$

then the Eq. (17) can be rewritten as:

$$\mathbf{s}_i(\mathbf{q}_i, \mathbf{w}_i, t) = k_{1i}\tilde{\mathbf{q}}_i + k_{2i}\tilde{\mathbf{w}}_i. \quad (20)$$

If the control action applied to the manipulator is able to keep the system trajectory on the sliding surface from some time  $t_s$ , as shown in the Fig. 1, Eq. (20) is identically zero:

$$\mathbf{s}_i(\mathbf{q}_i, \mathbf{w}_i, t) = k_{1i}\tilde{\mathbf{q}}_i + k_{2i}\tilde{\mathbf{w}}_i = 0. \quad (21)$$

Isolating  $\tilde{\mathbf{w}}_i$  gives:

$$\tilde{\mathbf{w}}_i = \dot{\tilde{\mathbf{q}}}_i = -\frac{k_{1i}}{k_{2i}}\tilde{\mathbf{q}}_i. \quad (22)$$

Therefore, from the time  $t_s$ , the position and velocity errors are going to converge exponentially to zero.

The rate of the system state convergence towards the sliding surface depends on the gain values  $k_{ji}$ , as shown by Eq. (22). The larger the gain  $k_{1i}$  (and smaller the gain  $k_{2i}$ ), the faster the convergence of the joint error  $i$  to zero. However, a faster convergence requires a larger control effort.

## Simulation Results

For a numeric simulation example, consider the robotic manipulator with two degrees of freedom (2 DOF) in a horizontal plane as shown in Fig. 4.

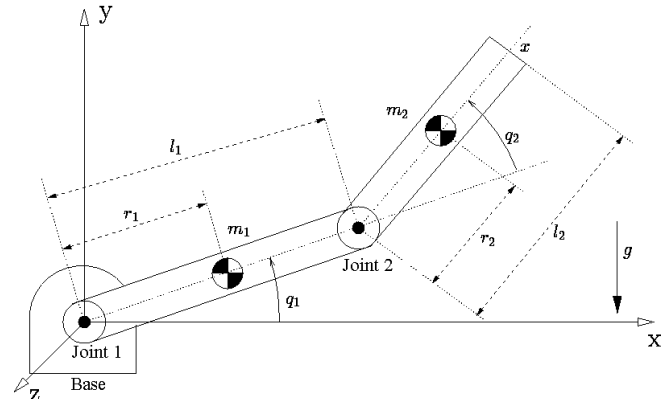


Figure 4. Robot Manipulator with Two Degrees of Freedom (2-DOF).

The following notation is used in this figure:

- $q_i$  - angular position of joint  $i$ , in radians;
- $l_i$  - length of link  $i$ , in meters;
- $r_i$  - distance between joint  $i$  and the center of mass of link  $i$ , in meters;
- $m_i$  - mass of link  $i$ , in kilograms;
- $I_i$  - moment of inertia of link  $i$  with respect to the axis that passes through the center of mass and is parallel to the  $z$  axis, in kilograms times squared meters.

The manipulator in Fig. 4 represents the links one and two of the SCARA manipulator shown in Fig. 5.

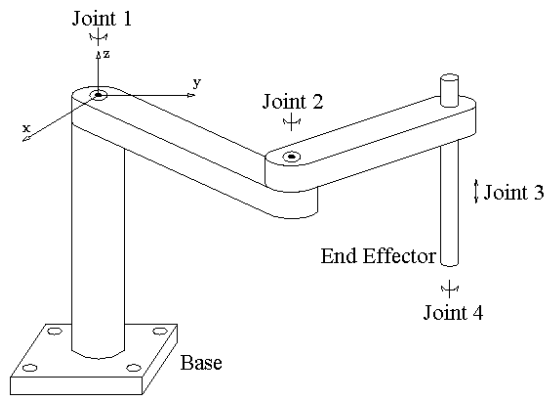


Figure 5. SCARA - Selective Compliance Assembly Robot Arm.

Although only joints one and two of the SCARA manipulator are used, all links must be considered in the modeling. Using the coordinate system shown in Fig. 5, two considerations are done in order regarding the dynamic model.

First, joints three and four are treated as being fixed. Thus, the last link represents a load to the manipulator's end effector, of mass  $m_L$  and moment of inertia  $I_L$ , which is associated with the axis that passes through the center of mass of link 2 and is parallel to the  $z$  axis.

The second consideration is that gravitational forces do not act on links one and two of the SCARA manipulator. Gravity is acting along the direction of the  $z$  axis (Fig. 5), so that it exerts no work in the directions where the manipulator can move. Thus, the gravitational forces vector  $G(q)$  is identically zero for all configurations of the manipulator.

The software Matlab<sup>®</sup> is used for the numeric simulation. The parameters of the industrial SCARA manipulator used in this work are presented at the Appendix.

The controller *sampling period* is 1.0 ms and the controller's parameters used are:

$$\begin{aligned}
 k_{11} &= 10.0 & ; & & k_{21} &= 1.0 & ; & & k_{12} &= 10.0 & ; & & k_{22} &= 1.0 \\
 u_{01} &= 70.0 \text{ Nm} & ; & & u_{02} &= 50.0 \text{ Nm} \\
 e_1 &= 0.05 & ; & & e_2 &= 0.15
 \end{aligned}
 \tag{23}$$

These values were obtained empirically (trial and error) after a few observations of the amplitude of the control signal and the reference tracking errors. Recently, the literature has been introducing methodologies based in adaptive control, neural networks and genetic algorithms applied to the tuning of classical and advanced controllers (Ambrosino, Celetano and Garofalo, 1984, Li et Al., 1996) that can be used here.

The initial and final positions  $q_b$  and  $q_e$  of the joints in the simulation are

$$q_b = \begin{bmatrix} 0 \\ 0 \end{bmatrix} \text{ rad} \quad ; \quad q_e = \begin{bmatrix} 2.0 \\ 1.5 \end{bmatrix} \text{ rad}
 \tag{24}$$

The position trajectories between initial and final points were obtained using an algorithm that generates a cubic polynomial interpolation. Each trajectory is a *mixed linear function with parables*. It has three parts: the initial and final parabolic parts, and the central part which is linear.

The position curves were obtained with acceleration of 4.0 rad/s<sup>2</sup> and maximum velocity of 3.0 rad/s for both joints. The velocities reached by the links are enough for the dynamic interactions between the two links to be significant, allowing the test of the robustness of the controller.

Figures 6 and 7 show, in dotted lines, the desired positions and velocities profiles, respectively. Simulation results are shown in continuous lines. The performance of the controller is good enough to make the profiles indistinguishable in the scale used for the plots.

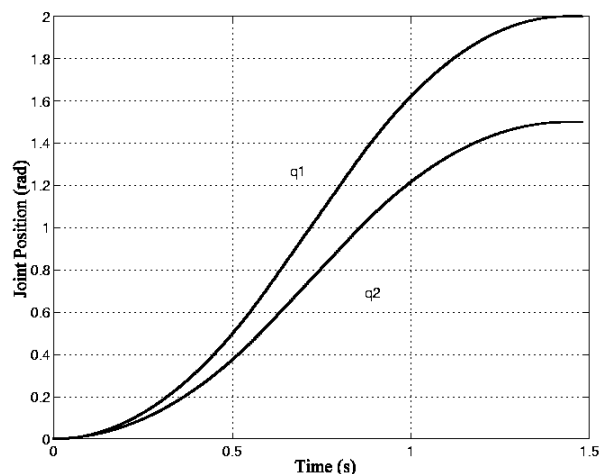


Figure 6. Simulation results: joint positions.

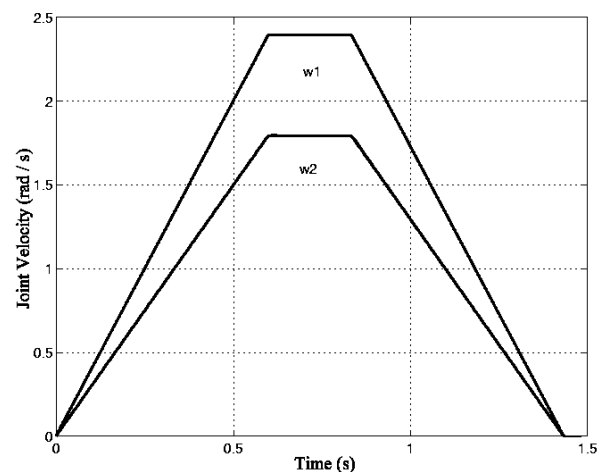


Figure 7. Simulation results: joint velocities.

For a better evaluation of performance, Figs. 8 and 9 display the corresponding errors. The maximum position errors are about  $2.0 \cdot 10^{-3}$  rad and the velocity errors are about  $2.0 \cdot 10^{-2}$  rad/s, showing

that the control keeps the errors small despite the use of a boundary layer

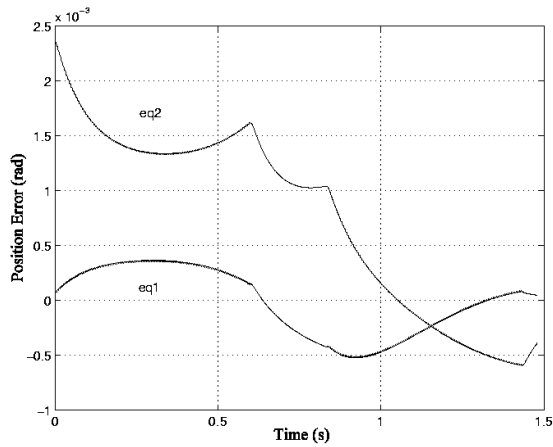


Figure 8. Simulation results: joint position errors.

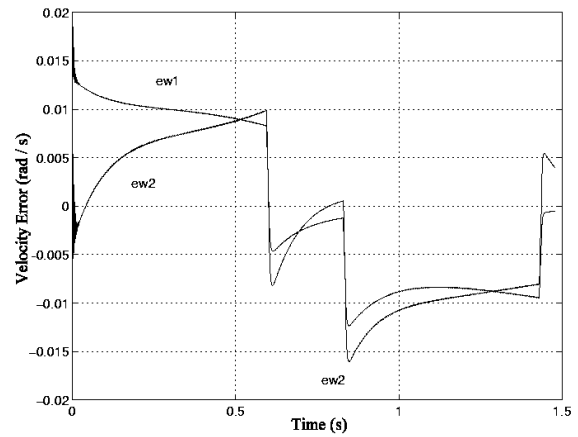


Figure 9. Simulation results: joint velocity errors.

Fig. 10 shows the sliding surface proximity, that is, the functions  $s_1(x,t)$  and  $s_2(x,t)$  on the boundary layer. Ideally, both functions should be identically zero. The deviations shown in the

plots are the result of the use of a boundary layer for avoidance of excessive chattering.

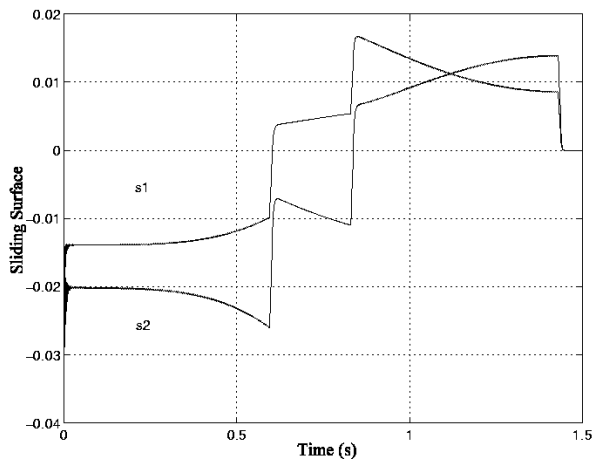


Figure 10. Simulation results: surface proximity.

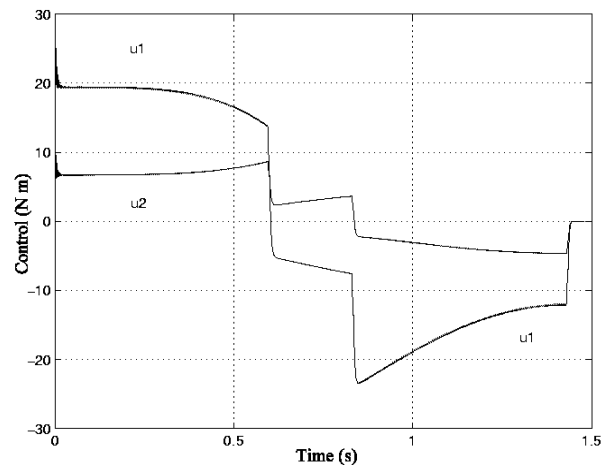


Figure 11. Simulation results: control signals.

Figure 11 shows the control applied in the robot manipulator. Note that it presents some significant chattering only at the beginning of the simulation and they are kept between maximum levels given by the controller's parameters, that are below the robot's limits used in the practical implementation (see the Appendix).

simulation) and the noisier environment given by the practical setup. The new values are:

$$e_1 = 0.10 \quad ; \quad e_2 = 0.30 . \quad (25)$$

### Implementation on an Industrial Robot

The same controller simulated numerically was implemented in XOboron (Reiser, 1991) to control an industrial SCARA whose model served as the basis for the simulation. On the practical experiment, basically the same controller's parameters (23) are used, including the sampling period (1.0 ms). The references are the same as those used in the simulation (Figs. 6 and 7). The only necessary adjustment is an increase in the boundary layers to accommodate for physical limitations of the actuators (not considered in the

The available physical parameters of the manipulator used in the simulation are not exact. Besides, frictions, flexibility and the actuators dynamics are not simulated. Thus, as expected, the results from the practical implementation are different from the simulation, as can be seen by the illustrations below.

Figures 12 and 13 show the positions and velocities profiles, respectively. The references are shown in dotted lines and the measured values in continuous lines. Tracking is still accomplished with good accuracy.

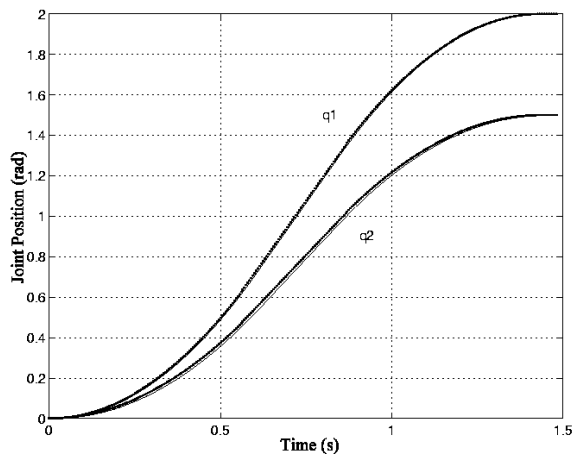


Figure 12. Experimental results: joint positions.

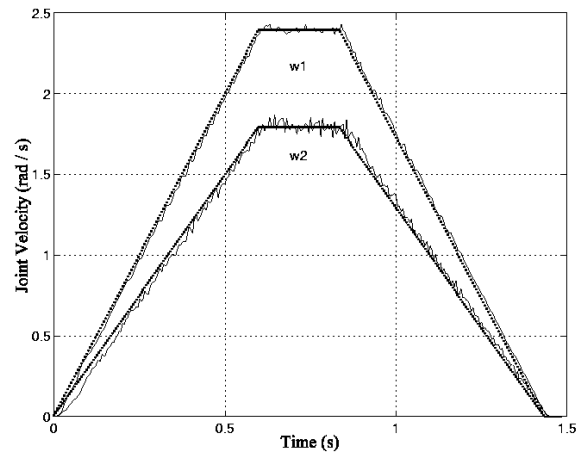


Figure 13. Experimental results: joint velocities.

Tracking errors are shown in Figs. 14 and 15. These errors are larger than the errors in the numeric simulation, due mainly to the fact that the boundary layer used here is greater than the one in the simulation.

Accuracy is good, and the errors in steady state are next to zero. The positions errors are on the range of  $2.0 \times 10^{-2}$  rad and the velocities errors are about  $1.0 \times 10^{-1}$  rad/s.

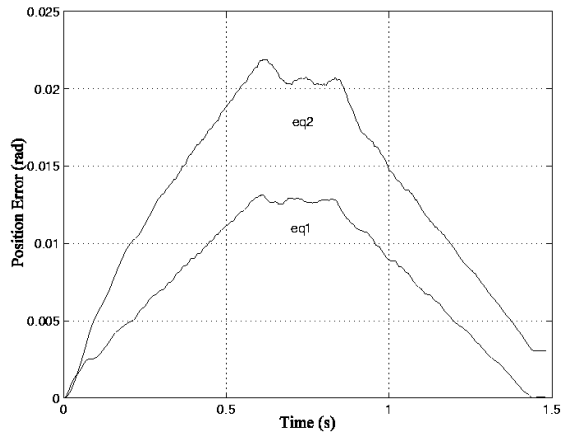


Figure 14. Experimental results: joint position errors.

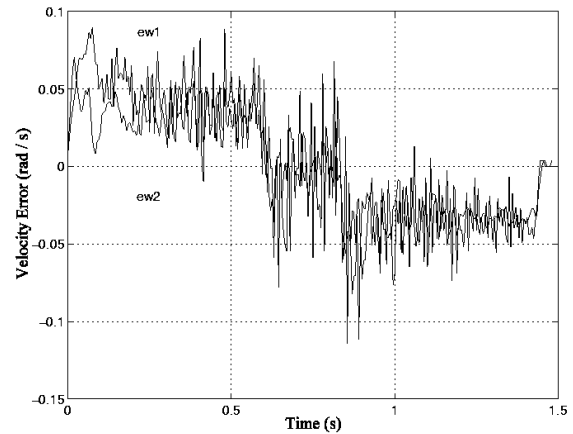
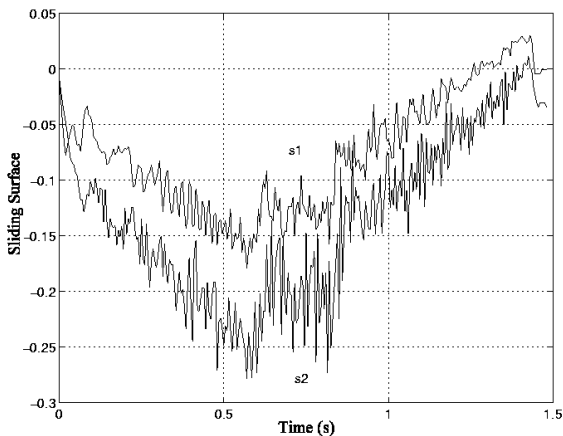


Figure 15. Experimental results: joint velocity errors.

Figure 16 shows the sliding surface proximity. The control signals are shown in Fig. 17. Again, the noisier situation faced in the practical implementation implies larger variations in the control signal. Another point of interest is the ever-positive control torque,

reflecting the “lagging” of the actual position along the trajectory. In the final half of the trajectory ( $t > 0.75$  s), the control effort is smaller since the error in velocity changes signal, meaning that a “braking” action is in order.



16. Experimental results: surface proximity.

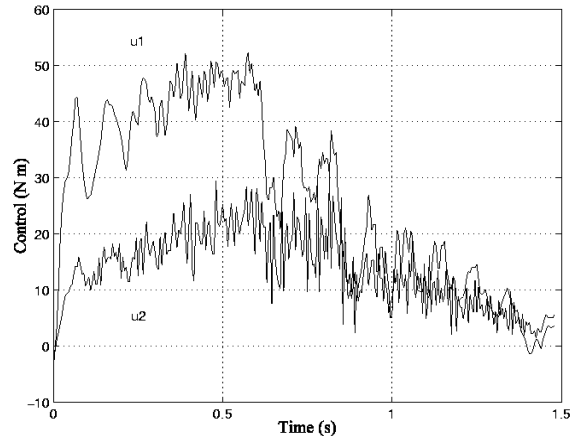


Figure 17. Experimental results: control signals.

## Conclusions

The use of a robust controller for the trajectory tracking of industrial manipulators with  $n$  degrees of freedom (DOF) was developed in this paper. The controller design was based on the theory of variable structure (VS) systems. Considering the theoretical development, a controller was designed and tested in simulation for a two DOF arm. Simulation results showed the excellence of the controller in following a timed path. This result led to the testing of the controller in an industrial arm, namely a two DOF SCARA manipulator. The aim has been to demonstrate the capabilities of such control method and its viability for practical use. Again, the results corroborated the theoretical development inasmuch as the performance obtained was well within the expected range of accuracy.

The robustness of VS control was demonstrated, as well as its advantages for applications in robot manipulators when the mathematical models that represent them with an adequate accuracy is not available—which is frequently the case. In the industrial arm used in this paper, for instance, no dynamic effect due to friction was considered in the model, and still the resulting performance in tracking the desired trajectory was very good.

The tuning of the controllers, so much in the simulation as in the practical implementation, was done empirically. Probably the best possible performance (response time, overshoot, etc.) was not reached. To repair this deficiency, further work can be done with techniques for automatic tuning that give optimum values for controller's parameters. However, in the authors' experience, trial-and-error tuning is adequate for producing performances with good accuracy, thanks to the robustness and convergence properties of VS control.

## Appendix

**Table A1. Dimensions and Masses of the SCARA Manipulator.**

Link $i$	Length $l_i$ (m)	Center of Mass $r_i$ (m)	Mass $m_i$ (kg)	Inertia $I_i$ (kg m <sup>2</sup> )
1	0.25	0.118	11.4	0.23
2	0.25	0.116	19.5	0.16
3	0.0	0.0	2.0	0.10
4	0.0	0.0	1.5	0.10

**Table A2. Limit Values of the SCARA Manipulator.**

Link $i$	Maximum Position	Minimum Position	Maximum Velocity	Maximum Torque
1	2.25 rad	-2.25 rad	3.0 rad/s	333.0 N m
2	1.90 rad	-1.90 rad	3.0 rad/s	157.0 N m
3	0.40 m	0.14 m	0.88 m/s	6.975 N m
4	2.50 rad	-2.50 rad	20.0 rad/s	16.74 N m

**Table A3. Time Constants of the Motors.**

Motor bls55	Motor bls72
joints two, three and four	joint one
mechanical: 1.7 ms	mechanical: 2.1 ms
electrical: 1.4 ms	electrical: 1.1 ms

## References

- Ambrosino, G., Celetano, G. and Garofalo, F., 1984, "Variable Structure Model Reference Adaptive Control Systems", *International Journal of Control*, vol. 39, no. 6, pp. 1339-1349.
- Asada, H. and Slotine, J-J. E., 1986, "Robot Analysis and Control", John Wiley & Sons Inc., New York, USA.
- Canudas, C., Siciliano, B. and Bastin, G., 1996, "Theory of Robot Control", Springer-Verlag, New York, USA.
- Craig, J. J., 1986, "Introduction to Robotics: Mechanics & Control", Addison-Wesley Publishing Company, USA.
- DeCarlo, R. A., Zak, S. H. and Matthews, G. P., 1988, "Variable Structure Control of Nonlinear Multivariable Systems: A Tutorial", *Proc. of the IEEE*, vol. 76, no. 3, pp. 212-232, March.
- Doyle, J.C., K. Glover, P. Khargonekar, B.A. Francis; "State-Space Solutions to Standard H<sub>2</sub> and H<sub>∞</sub> Control Problems". *IEEE Transactions on Automatic Control*, vol. 34, pp. 831-847, 1989.
- El-Khazali, R. and DeCarlo, R., 1995, "Output Feedback Variable Structure Control Design, *Automática*, vol. 31, no. 6, pp. 805-816.
- Filippov, A. F., 1964, "Differential Equations with Discontinuous Right Hand Sides", *Am. Math. Soc. Transl.*, vol. 42, pp. 199-231.
- Fu, L.-C. and Liao, T.-L., 1990, "Globally Stable Robust Tracking of Nonlinear Systems Using Variable Structure Control and with an Application to a Robotic Manipulator", *IEEE Transactions on Automatic Control*, vol. 35, no. 12, pp. 1345-1350, December.
- Gao, W., Wang, Y. and Homaifa, A., 1995, "Discrete-Time Variable Structure Control Systems", *IEEE Transactions on Industrial Electronics*, vol. 42, no. 2, pp. 117-122, April.
- Lewis, F. L., Abdallah, C. T. and Dawson, D. M., 1993, "Control of Robot Manipulators", Macmillan Publishing Company, New York, USA.
- Li, Y., Ng, K. C., Murray-Smith, D. J., Gray, G. J. and Sharman, K., 1996, "Genetic Algorithm Automated Approach to the Design of Sliding Mode Control Systems", *International Journal of Control*, vol. 63, no. 4, pp. 721-739.
- Reiser, M., 1991, "The Oberon System: user guide and programmer's manual", Addison-Wesley Publishing Company, New York, USA.
- Slotine, J-J. E. and Li, W., 1991, "Applied Nonlinear Control", Prentice Hall, New Jersey, USA.
- Utkin, V. I., 1977, "Variable Structure Systems with Sliding Modes", *IEEE Transactions on Automatic Control*, vol. AC-22, no. 2, pp. 212-222, April.
- Utkin, V. I., 1983, "Variable Structure Systems: Present and Future", *Automation and Remote Control*, vol. 44, no. 9, pp. 1105-1120, September.
- Utkin, V. I., 1992, "Sliding Modes in Control Optimization", Springer-Verlag, New York, USA.
- Wolovich, W.A., 1995, "Automatic Control Systems: Basic Analysis and Design", Saunders College Publishing, USA.